Toroidal ripple transport of beam ions in the mega-ampère spherical tokamak

K. G. McClements and M. J. Hole

Citation: Physics of Plasmas (1994-present) **19**, 072514 (2012); doi: 10.1063/1.4737605
View online: http://dx.doi.org/10.1063/1.4737605
View Table of Contents: http://scitation.aip.org/content/aip/journal/pop/19/7?ver=pdfcov
Published by the AIP Publishing

Toroidal ripple transport of beam ions in the mega-ampère spherical tokamak

K. G. McClements[1] and M. J. Hole[2]
[1]*EURATOM/CCFE Fusion Association, Culham Science Centre, Abingdon, Oxfordshire OX14 3DB, United Kingdom*
[2]*Plasma Research Laboratory, Research School of Physical Science and Engineering, Australian National University, Canberra, ACT 0200, Australia*

(Received 30 April 2012; accepted 27 June 2012; published online 20 July 2012)

The transport of injected beam ions due to toroidal magnetic field ripple in the mega-ampère spherical tokamak (MAST) is quantified using a full orbit particle tracking code, with collisional slowing-down and pitch-angle scattering by electrons and bulk ions taken into account. It is shown that the level of ripple losses is generally rather low, although it depends sensitively on the major radius of the outer midplane plasma edge; for typical values of this parameter in MAST plasmas, the reduction in beam heating power due specifically to ripple transport is less than 1%, and the ripple contribution to beam ion diffusivity is of the order of 0.1 m^2 s^{-1} or less. It is concluded that ripple effects make only a small contribution to anomalous transport rates that have been invoked to account for measured neutron rates and plasma stored energies in some MAST discharges. Delayed (non-prompt) losses are shown to occur close to the outer midplane, suggesting that banana-drift diffusion is the most likely cause of the ripple-induced losses. [http://dx.doi.org/10.1063/1.4737605]

I. INTRODUCTION

The transport modelling of tokamak plasmas is often based on the premise that the confinement of highly suprathermal ions, whether originating from fusion reactions, radio-frequency wave heating, or neutral beam injection (NBI), is determined solely by the axisymmetric component of the equilibrium magnetic field and Coulomb collisions. In such cases, the confinement is described as classical. It is well-established that the transport of bulk (thermal) ions and electrons is due predominantly to turbulence, but ions of sufficiently high energy are commonly assumed to undergo little or no turbulent transport. The basis for this assumption is that the Larmor radii of such particles exceed the typical wavelengths of turbulent fields, which thus average to a value close to zero over a single gyration.[1] Similar arguments have been advanced to suggest that energetic ions are unlikely to be significantly affected by the presence of short wavelength magnetohydrodynamic (MHD) modes.[2] On the other hand, energetic ions are potentially susceptible to non-classical transport due to toroidal ripple in the equilibrium magnetic field, which is an unavoidable consequence of the discrete nature of the toroidal field coils.[3] In general, it is found that ripple-induced transport is very sensitive to the amplitude of the ripple perturbations to the magnetic field, which in turn depends on the number of toroidal field coils and their distance from the plasma.

As noted by Hinton[4] and Putvinskii,[5] cyclotron resonance with ripple field perturbations can give rise to additional ripple transport and loss, over and above that described by guiding centre calculations. The resonance condition for a static field perturbation, such as toroidal ripple, is[6]

$$k_{\|} v_{\|} = \Omega_i, \tag{1}$$

where $k_{\|}$ is the component of the ripple perturbation wave vector parallel to the magnetic field, $v_{\|}$ is the parallel component of the particle velocity, and Ω_i is its cyclotron frequency. The ripple wavelength is of the order of R/N, where R is distance from the tokamak symmetry axis and N is the number of coils. Hence, cyclotron resonance occurs if $\rho \equiv v_{\|}/\Omega_i$ is approximately equal to R/N. For ions of a particular energy, this resonance is more likely to occur in spherical tokamaks than conventional tokamaks, since magnetic fields are typically much smaller in the former than in the latter.[7] Plasmas in the mega-ampère spherical tokamak (MAST) are heated using deuterium neutral beams, the deuterons having energies of up to about 70 keV when they first appear as ions in the plasma. The toroidal magnetic field in MAST is no higher than 0.52 T at the magnetic axis, located at $R \simeq 0.85$ m, and is produced by currents in $N = 12$ rectangular-shaped coils. For a 70 keV beam deuteron in MAST, $\rho \sim R/N \sim 0.1$ m. Hence, the conditions for a particle-ripple cyclotron resonance are approximately satisfied, and on this basis it appears possible that the ripple transport of energetic beam ions could be significantly enhanced as a result of finite Larmor radius effects.

In the present paper, we use a full orbit particle tracking code to quantify ripple transport of beam ions in MAST. One motivation for this study is that anomalous (i.e., non-classical) transport of beam ions, corresponding to particle diffusivities in the range 0.5–3.0 m^2 s^{-1}, has recently been invoked to account for experimentally-measured neutron rates and stored plasma energies in MAST.[8,9] While there is some evidence of a correlation between high rates of beam ion transport and MHD activity, it is unclear whether the anomalous transport is due mainly to such activity; it is also possible that either turbulence or toroidal ripple could be affecting beam ion confinement. The contribution of ripple effects to beam ion transport is likely to be sensitive to the

location of the outer plasma boundary R_{edge}, since this determines how close the plasma is to the coils and hence the ripple amplitude inside the plasma. Since MAST plasmas are invariably much smaller than the vacuum vessel containing them, a wide range of values of R_{edge} are in principle possible. It is therefore worthwhile to address the issue of how large MAST plasmas can be before ripple losses become unacceptably large. After quantifying the ripple perturbations to the MAST equilibrium field in Sec. II, we present in Sec. III results obtained by tracking the full orbits of beam ions in MAST-like plasmas, taking account of both ripple and collisions. We discuss the significance of these results in Sec. IV.

II. TOROIDAL RIPPLE IN MAST

We assume that the ripple perturbation to the toroidal magnetic field $\tilde{B}_\varphi$ has a single, dominant toroidal harmonic and define a dimensionless ripple amplitude δ by the expression[6]

$$\tilde{B}_\varphi = \frac{B_0 R_0}{R}\delta(R,Z)\cos(N\varphi), \tag{2}$$

where Z is the vertical distance, B_0 is the vacuum toroidal field at the magnetic axis ($R = R_0, Z = 0$), and φ is the toroidal angle. The toroidal field coils on the outside of the MAST vacuum vessel are exactly vertical over the entire vertical extent of the plasma, with the result that the contours of constant ripple amplitude within the plasma also have this symmetry.[10] Specifically, it can be shown that the ripple amplitude within the plasma is well-approximated by the expression[7]

$$\delta = \left(\frac{R}{R_{coil}}\right)^N, \tag{3}$$

where R_{coil} is the mean major radius of the outer vertical legs of the toroidal field coils. The toroidal field perturbation thus becomes

$$\tilde{B}_\varphi = \frac{B_0 R_0}{R}\left(\frac{R}{R_{coil}}\right)^N \cos(N\varphi), \tag{4}$$

and, since the total magnetic field **B** must be divergence-free, there is a also a radial field perturbation

$$\tilde{B}_R = \frac{B_0 R_0}{R}\left(\frac{R}{R_{coil}}\right)^N \sin(N\varphi). \tag{5}$$

With these perturbations included in the total field, the Hamiltonion of a single charged collisionless particle depends explicitly on φ and hence the toroidal canonical momentum P_φ is not an exact constant of its motion. Such particles are potentially subject to collisionless radial transport. Ripple transport is further enhanced by collisional pitch angle scattering.[3]

In the case of MAST, $R_{coil} \simeq 2.09$ m and, as discussed previously, $N = 12$. With these parameters, the ripple amplitude given by Eq. (3) at the outer midplane edge of a typical MAST plasma ($R_{edge} \simeq 1.45$ m) is approximately 1.2%. This is comparable to the projected maximum ripple amplitude on the last closed flux surface of plasmas in the proposed ITER device, which has been predicted to cause fusion α-particle losses of between 2% and 20%, depending on the magnetic shear profile.[11] This, combined with the cyclotron resonance effects discussed in Sec. I, suggests that the ripple in MAST could be sufficiently large to cause significant transport and loss of beam ions, with a consequent loss of beam heating and current drive efficiency.

Some indication of what to expect in MAST is provided by a numerical study[7] of collisionless ripple losses of fusion α-particles from a proposed spherical tokamak component test facility (CTF).[12] In a series of simulations, the assumed number of toroidal field coils was varied from $N = 7$ to $N = 20$, the maximum ripple amplitude within the plasma varying from 0.8% to 0.0001%. Despite this large variation the computed loss rates for N ranging from 9 to 20 were found to be statistically indistinguishable (and well above the prompt rate), suggesting that the losses were being enhanced by finite Larmor radius effects, arising from either the ripple resonance given by Eq. (1) or violation of magnetic moment (μ) conservation in the axisymmetric component of the magnetic field. The latter interpretation is supported by the fact that ripple effects would be expected to be completely negligible in the case of $N = 20$, irrespective of whether Eq. (1) were satisfied or not. Violation of μ conservation is generally associated with large values of $\rho^* \equiv \rho/R$, which has similar values (~ 0.1) for fusion α-particles in CTF and 65 keV beam ions in MAST. On the other hand, the ripple amplitude is about 20 times higher in MAST, and so one might expect ripple resonance effects on fast ion transport to be more significant.

III. PARTICLE SIMULATIONS

A. Modelling of collisions

As noted previously, ripple transport can be significantly enhanced by collisions. In principle, this process can be described using a suitable Fokker-Planck equation;[13] in the present paper, we instead track individual full particle orbits, taking collisions into account. The culham energy-conserving orbit (CUEBIT) code[14] has recently been modified to include the collisional interaction of suprathermal test-particles with a Maxwellian population of field particles. In particular, the anisotropic character of this interaction (random accelerations due to collisions with more slowly-moving field particles are typically greater in directions orthogonal to the instantaneous velocity vector **v** of the particle than they are along **v**[15]) has been incorporated into the code. This is necessary in order to model accurately the slowing-down and transport of beam ions in tokamaks, since they are typically born with energies in the tens or hundreds of keV range in plasmas with ion temperatures no greater than about 10 keV. CUEBIT is used to solve the Lorentz force equation in cartesian coordinates that are fixed in the laboratory; the random accelerations in the three cartesian directions can be related to those parallel ($a_\parallel$) and perpendicular ($\mathbf{a}_\perp$) to **v** by a rotation matrix. The quantities $a_\parallel$ and $\mathbf{a}_\perp$ are sampled from Gaussian distributions with zero means and variances determined by the requirement that

the set of stochastic orbit equations solved using the code be equivalent to the appropriate Fokker-Planck equation.[16] We may write the collision terms in this equation in the form

$$\left(\frac{\partial f}{\partial t}\right)_{\text{coll}} = \frac{\partial}{\partial \mathbf{v}} \cdot \left[\mathbf{A} f + \frac{\partial}{\partial \mathbf{v}} \cdot (\mathsf{D} f) \right], \tag{6}$$

where f is the distribution function of the test-particle species, and the components of the friction vector $\mathbf{A}$ and the diffusion tensor D depend only on the prescribed parameters of a field particle distribution. Using cartesian velocity space coordinates, with the x-direction taken to be parallel to $\mathbf{v}$, the diffusion tensor has the following non-zero components for the case of collisions between suprathermal hydrogenic beam ions and Maxwellian bulk ions of the same species with zero mean flow:[17]

$$D_{xx} = \frac{n_i e^4 \ln\Lambda}{4\pi\epsilon_0^2 m_i^2 v} G(v/v_i), \tag{7}$$

$$D_{yy} = D_{zz} = \frac{n_i e^4 \ln\Lambda}{8\pi\epsilon_0^2 m_i^2 v} [\phi(v/v_i) - G(v/v_i)], \tag{8}$$

where n_i is the bulk ion density, e is the proton charge, $\ln\Lambda$ is the Coulomb logarithm, ϵ_0 is free space permeability, m_i is the ion mass, v is the test-particle speed, $v_i = (2T_i/m_i)^{1/2}$ where T_i is bulk ion temperature, ϕ is the error function and

$$G(x) = \frac{\phi(x) - x\phi'(x)}{2x^2}. \tag{9}$$

If the orbit equation is approximated by a finite difference equation with time step δt, it is straightforward to show from the standard theory of stochastic differential equations[16] that the required variances of the parallel and perpendicular random accelerations are given by

$$\langle a_\parallel^2 \rangle = \frac{3\sqrt{\pi}}{2\tau\delta t} \frac{v_i^3 G(v/v_i)}{v}, \tag{10}$$

$$\langle a_\perp^2 \rangle = \frac{3\sqrt{\pi}}{2\tau\delta t} \frac{v_i^3 [\phi(v/v_i) - G(v/v_i)]}{v}, \tag{11}$$

where

$$\tau = \frac{3\pi^{3/2}\epsilon_0^2 m_i^2 v_i^3}{n_i e^4 \ln\Lambda}, \tag{12}$$

is a velocity-independent collision time. In the limit $v/v_i \to 0$, these expressions reduce to $\langle a_\parallel^2 \rangle = \langle a_\perp^2 \rangle/2 = v_i^2/(\tau\delta t)$, which are the appropriate variances for test-particles whose speeds are lower than the thermal speed of the species with which they are colliding.[18]

The slowing-down rate due to collisions with bulk ions is given by[17]

$$\nu_s = \frac{n_i e^4 \ln\Lambda G(v/v_i)}{\pi\epsilon_0^2 m_i^2 v_i^2 v}. \tag{13}$$

We take this process into account in our simulations, together with slowing-down due to collisions with electrons and random accelerations due to collisional interactions with this species. However, we neglect the possibility of beam ions being lost due to charge-exchange with neutral atoms.

For the purpose of modelling the collision processes described above, the plasma temperature was assumed to have the same value for bulk ions and electrons, and to vary linearly with poloidal flux from 1.3 keV at the magnetic axis to 100 eV at the last closed flux surface. To approximate conditions in typical MAST plasmas with co-current NBI (see, e.g., Fig. 4 in Ref. 8), the plasma density profile was assumed to be somewhat flatter, varying as the square root of poloidal flux (defined as zero at the magnetic axis and increasing monotonically to the plasma edge), and ranging from 3×10^{19} m^{-3} at the axis to 10^{18} m^{-3} at the edge.

In the collisionless limit and in the absence of electric fields, particle energy is always conserved to machine accuracy in CUEBIT, whereas P_φ is conserved (in the case of axisymmetric equilibria) to an accuracy that depends on the choice of $\Omega_i \delta t$. In making this choice care must be taken to ensure that changes in P_φ are due principally to either collisions or ripple rather than truncation error in the orbit-following algorithm. Since, for comparison purposes, we will present results from simulations with zero ripple, the requirement is that the departure of P_φ from its initial value due to collisions alone should exceed that due to truncation error. It is apparent from the definition of collisional slowing-down time τ_{slow} that in a finite time interval Δt, there is a collisionally-induced change in toroidal velocity v_φ given by $\Delta v_\varphi \sim (\Delta t/\tau_{\text{slow}}) v_\varphi$. Now, $P_\varphi = m_i R v_\varphi + e\psi$ where ψ is the poloidal flux (defined such that the poloidal magnetic field is $\nabla\psi \times \nabla\varphi$), and beam ion energies in MAST are such that the two terms in P_φ are comparable in magnitude. It follows that collisionally-induced changes in P_φ are given approximately by

$$\frac{\Delta P_\varphi}{P_\varphi} \sim \frac{\Delta t}{\tau_{\text{slow}}}. \tag{14}$$

Slowing-down times in MAST are typically a few tens of milliseconds. Tracking collisionless beam ion orbits in axisymmetric MAST-like equilibria for 50 ms, we found that P_φ was conserved to an accuracy of about one part in 10^4 when δt was set equal to 3% of a cyclotron period, but the numerically-induced values of $\Delta P_\varphi/P_\varphi$ over the same timescale were found to approach unity when δt was increased to 10% of $2\pi/\Omega_i$. For this reason, all of the simulations reported in this paper were performed with $\Omega_i \delta t/2\pi = 0.03$.

B. Results

CUEBIT was used to track the full orbits of beam ions with a range of initial energies up to about 65 keV in a model MAST equilibrium comprising an axisymmetric component, computed using a Grad-Shafranov solver named GS2D[19] and the ripple fields given by Eqs. (4) and (5). For this equilibrium, the plasma current is 726 kA and $B_0 = 0.43$ T. Figure 1 is a vertical view of the beam deposition profile used in the

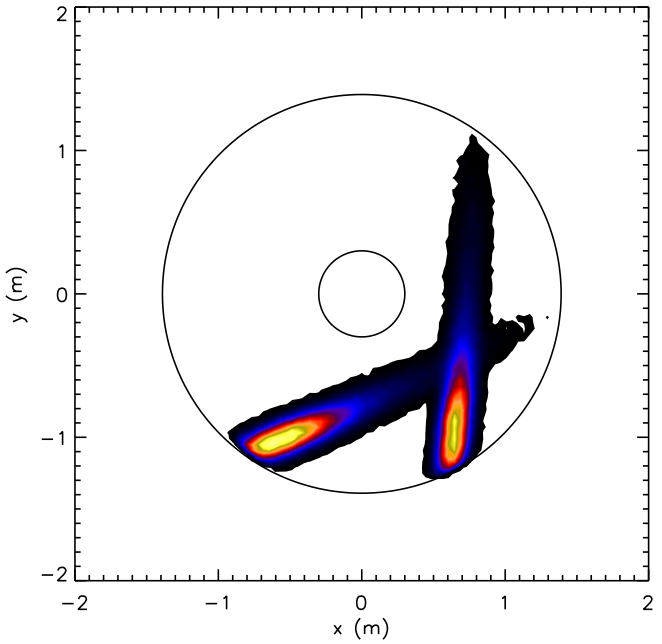

FIG. 1. Distribution of beam ion birth positions viewed from above the midplane in a typical MAST discharge, with the highest birth probability indicated in yellow. The circles indicate the inner and outer plasma boundaries in the midplane.

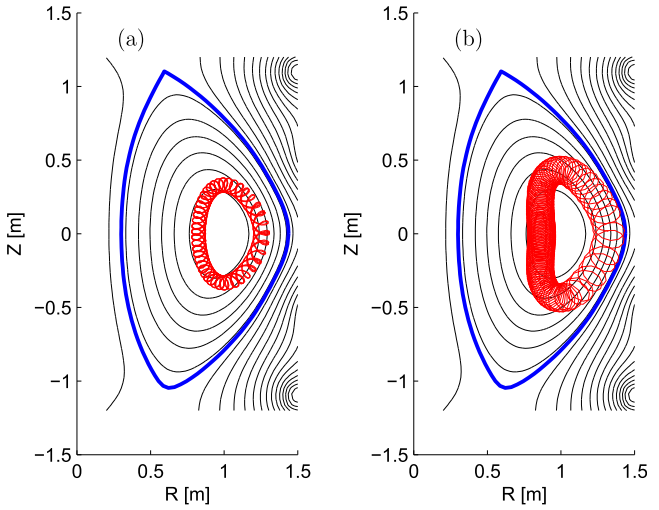

FIG. 2. Projections onto the poloidal plane of collisionless beam ion orbits in MAST. The ions were born at (a) $R = 0.81$ m, $Z = 0.12$ m and (b) $R = 1.32$ m, $Z = 0.02$ m. Black curves show flux surface contours, with the last closed flux surface in blue.

simulations, with colors from black to yellow indicating increasing birth probability. The inner and outer midplane plasma boundaries are also shown in this figure. There are in fact two beams, with the center of each beamline tangential to an equilibrium flux surface passing through $R \simeq 0.7$ m, $Z \simeq 0$, although experiments have been performed with the plasma shifted vertically so that the center of the beamline lies below or above the plasma midplane.[8] The plasma density profile in MAST is such that the majority of beam atoms are ionized well before they reach the tangency radius, and in fact many are born within a few centimeters of the outer plasma edge. Such particles encounter a relatively high ripple amplitude, and moreover are susceptible to being lost from the plasma in the presence of either collisions or ripple. This point is illustrated by Fig. 2, which shows the projections onto the poloidal plane of the collisionless orbits of beam ions that are (a) well-confined and (b) marginally-confined. In computing these orbits, the ripple contributions to the magnetic field were neglected. Figure 2 indicates the extent of the poloidal cross-section sampled by some beam ions immediately after their appearance in the plasma, and also the fact that these particles typically have Larmor radii that are a significant fraction of the plasma minor radius. In general, the beam ion deposition profile extends up to the plasma edge.

The beam ions whose orbits were tracked in the simulations were born with velocity vectors directed along the beamlines indicated in Fig. 1, and an energy distribution consisting essentially of six delta-functions at energies $E_1 \simeq 65$ keV, $E_2 \simeq 51$ keV, $E_1/2$, $E_2/2$, $E_1/3$, and $E_2/3$. Birth energies that are fractions of the highest value for each injector (E_1 and E_2) result from the breakup of diatomic and triatomic ions, which are always present to some extent in the beam injector system;[20] however, most of the beam ions in the simulations were born at the highest two energies.

The effect of toroidal ripple on beam ion confinement in the model MAST equilibrium was quantified by launching a total of $N_0 = 28\,000$ test-particles, sampled randomly from the deposition profile shown in Fig. 1, tracking their orbits for several tens of milliseconds, and recording as a function of time the number of particles remaining in the plasma $N_b(t)$, with and without toroidal ripple taken into account. A particle was considered to be lost if it crossed the last closed flux surface at any point on its trajectory. The results are shown in Fig. 3. The divergence of the solid curve (finite ripple) from the dashed curve (zero ripple) makes it clear that ripple effects are causing a measurable degradation in confinement. At the end of the simulations, the cumulative additional particle losses due to ripple amount to approximately $(0.7 \pm 0.1)\%$ of N_0 (separate simulations were in fact carried

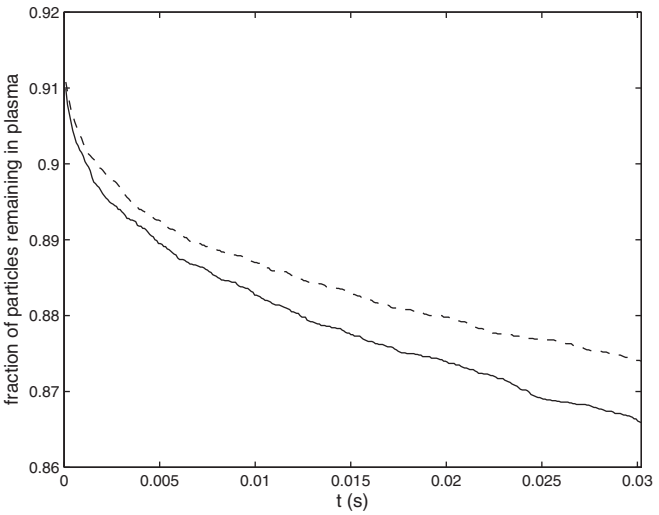

FIG. 3. Number of beam ions remaining in the plasma N_b as a function of time with (solid curve) and without (dashed curve) toroidal ripple taken into account, and with $R_{edge} = 1.44$ m.

out with three independently-chosen sets of initial particle parameters; the estimated error in the cumulative ripple loss is based on a comparison between results obtained with and without ripple for these three parameter sets).

The decay rate of N_b provides a simple measure of the confinement time τ_c in the two cases. Defining a confinement time τ_c by writing $N_b(t) = N_0(1 - t/\tau_c)$, we infer from Fig. 3 that

$$\tau_c = 237\,\text{ms}, \tag{15}$$

when the transport is determined solely by collisions, and

$$\tau_c = 224\,\text{ms}, \tag{16}$$

when ripple transport is also taken into account. While both values of τ_c are broadly consistent with classical confinement, the ripple value is significantly lower than the no-ripple value. In view of the large ρ^* of the beam ions, their transport is unlikely to be purely diffusive. We can, however, make a rough estimate of the average effective beam ion diffusivity D_b by taking the MAST minor radius $a \simeq 0.65\,\text{m}$ to be a diffusive length scale, so that $D_b \sim a^2/\tau_c$. Evaluating this quantity for the confinement times given in Eqs. (15) and (16), and taking the difference, we estimate the anomalous diffusivity due to ripple transport to be

$$D_b^{\text{ripple}} \sim 0.1\,\text{m}^2\text{s}^{-1}. \tag{17}$$

This is significantly lower than the anomalous diffusivity found by Turnyanskiy, Valovič and co-workers[8,9] to be required to explain experimental results in MAST (0.5–3.0 $\text{m}^2\,\text{s}^{-1}$), and in fact it is likely to be an overestimate since the distance from the center of the beam deposition profiles to the plasma edge is smaller than a (cf. Fig. 1). We deduce that, at most, only a small fraction of the anomalous transport deduced in Ref. 8 is attributable to toroidal ripple.

Further information on the interplay between collisions and ripple effects can be obtained by computing the energy distributions of the lost ions. Specifically, the energies of the lost ions were recorded and binned in 3.3 keV intervals up to 70 keV; the results are shown in Fig. 4. The highest number of losses occurs promptly, on sub-collisional timescales, and thus occurs close to the birth energies. Differences between the distributions with and without ripple taken into account are most apparent when the beam ions have slowed down to energies substantially below the birth energies (in particular the primary birth energies of 51 keV and 65 keV), suggesting that collisional effects are contributing to the ripple transport.[3]

The (R, Z) coordinates of each particle at the point where it crossed the last closed flux surface were also recorded, enabling us to plot the poloidal distribution of the losses, as shown in Fig. 5. For the purpose of generating this figure, the poloidal angle was defined as $\theta \equiv \tan^{-1}[Z/(R - R_0)]$. No losses at all occurred inboard of the magnetic axis, which is why the range of poloidal angles in Fig. 5 is restricted to $-90^\circ < \theta < 90^\circ$. There are two distinct peaks in each distribution, one above the midplane and centered on $\theta \simeq 30^\circ$, the other having a maximum close to the midplane. Only in the latter case do we see significant differences between the simulations with ripple (solid curve) and without ripple (dashed curve). The peak above the midplane is due mainly to prompt (first orbit) losses of beam ions born close to the last closed flux surface, which occur too rapidly for either collisions or toroidal ripple have any significant effect. Non-prompt losses, on the other hand, occur due to the combined effects of collisions and ripple.

It is significant that the ripple enhancement of the non-prompt losses (indicated by the difference between the curves in Fig. 5) also peaks close to the midplane, because this suggests that ripple trapping is not contributing to the loss rate. Ripple-trapped particles are generally lost rapidly from the plasma due to a vertical drift in the grad-B drift direction,[3] which is downward in the case of the equilibrium used in our simulations. Thus if ripple-trapping were occurring to any significant extent, we would expect to see additional losses in the ripple case occurring well below the midplane. The fact that no such losses are observed, whereas

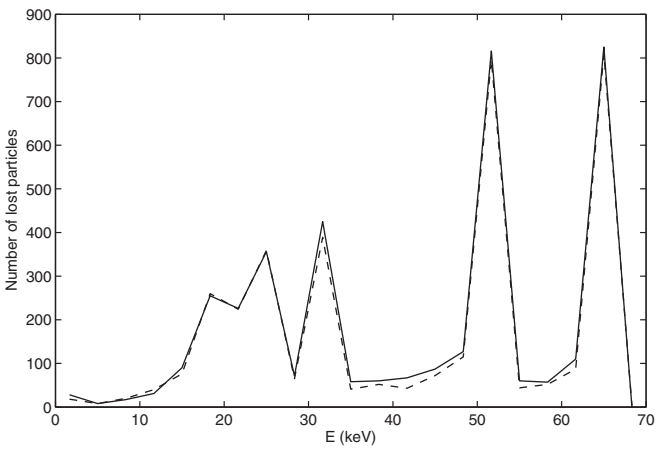

FIG. 4. Energy distributions of lost particles with (solid curve) and without (dashed curve) toroidal ripple taken into account, and with $R_{\text{out}} = 1.44\,\text{m}$.

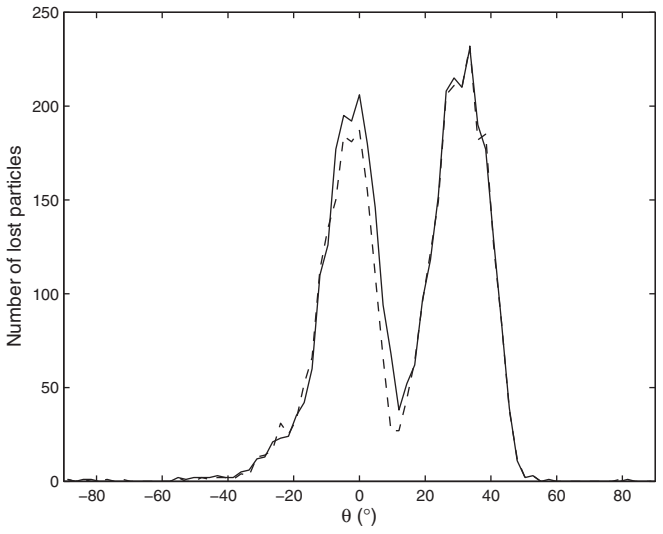

FIG. 5. Poloidal distributions of lost particles with (solid curve) and without (dashed curve) toroidal ripple taken into account, and with $R_{\text{edge}} = 1.44\,\text{m}$.

we do observe a ripple-induced enhancement in the losses close to the midplane, implies that banana-drift diffusion may be playing a role.[3] This arises from an oscillation in particle poloidal velocities $\dot{\theta}$ induced by $\tilde{B}_\varphi$, which in turn causes an oscillation in the bounce position of trapped particles, and hence in the maximum radial excursion of the particle. As in the case of an unperturbed trapped orbit, the maximum excursion occurs in the outer midplane, and so this is where any losses tend to peak. A diffusion coefficient describing this process is derived in Ref. 3; this is not directly applicable to the simulations described here, since it requires that collisions are sufficiently rapid to decorrelate the ripple phase at successive trapped particle bounces (the "ripple-plateau" regime). The collision rate of energetic beam ions in MAST is too low for this condition to apply. However, even an oscillatory (non-diffusive) motion of the maximum radial excursion would be expected to give rise to particle losses if the unperturbed orbits are already close to the plasma boundary; it is evident from Figs. 1 and 2 that this is the case in our simulations.

Further evidence for this interpretation of the losses is provided by Fig. 6, in which the poloidal angle and energy of each lost particle are recorded at the instant it crosses the last closed flux surface. The dense vertical lines on this plot, at the birth energies of the various beam components, arise from the prompt losses discussed above; these occur most frequently above the midplane, although some prompt losses are also observed at $\theta \lesssim 0°$, particularly at the highest injection energies. In contrast, most of the delayed losses (indicated by points lying between the birth energies) occur close to the midplane. The fact that so many of the losses are prompt may help to explain the low level of ripple losses from a plasma with a relatively high ripple amplitude ($\sim 1\%$) at the outer midplane edge: the beam ions that are born close enough to the edge to encounter the highest ripple field have large normalised Larmor radii (cf. Fig. 2(b)) and are consequently lost promptly whether the ripple is present or not. Those that are left encounter a significantly smaller ripple field, on average, and are thus subject to a relatively low level of ripple transport. This effect is likely to be further enhanced by charge-exchange losses, which also become increasingly likely to occur towards the plasma edge.

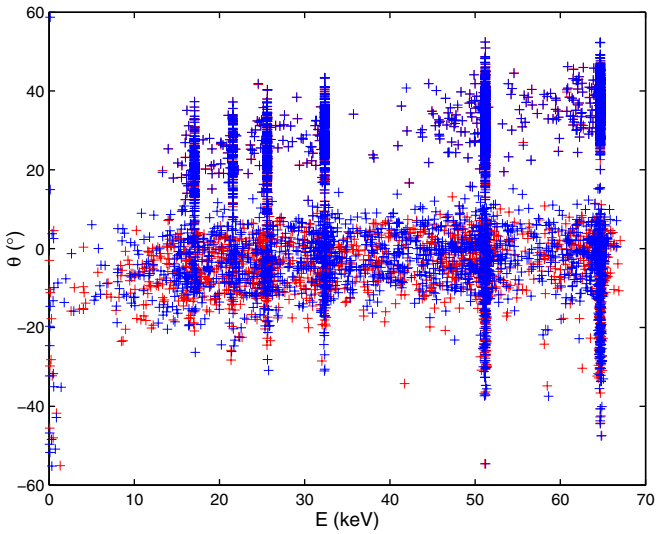

FIG. 6. Poloidal angle versus energy of lost particles with (blue crosses) and without (red crosses) toroidal ripple taken into account, and with $R_{edge} = 1.44$ m.

In a plasma with perfect collisional confinement, energetic particles would be completely thermalised within the plasma, and would then be lost slowly through neoclassical processes. Since initial fast ion energies are, by definition, much higher than thermal energies, the fraction of beam heating power lost from the plasma due to collisional and ripple transport can be estimated very easily by summing the energies of lost particles when they cross the last closed flux surface, and dividing this by the aggregate initial energy of all the simulated particles. Performing these calculations for the simulations described above, and subtracting the figure for the ripple case from that obtained without ripple, we estimate the ripple-induced power loss fraction to be approximately 0.8%. However, as noted previously, ripple transport is generally found to be very sensitive to the distance between the plasma and the toroidal field coils. To gauge this sensitivity, we have carried out a set of longer simulations, each covering a period of approximately 90 ms, using the equilibrium described above, and equilibria that are modified by decreasing and increasing the major radii by about 5%, giving three different values of R_{edge}. The values of poloidal flux and RB_φ, where B_φ is the equilibrium toroidal magnetic field, were left unchanged, but the plasma safety factor q was slightly modified. The major radii of the beam ion birth positions were also rescaled to ensure in each case that the model deposition profile extended to the plasma edge. In each case, 10,000 test particles were simulated. As before, simulations were performed with and without ripple, and the ripple-induced power loss fraction estimated. Results obtained for the three values of R_{edge} are listed in Table I. We note that increasing the plasma size by a few centimetres can increase the power loss fraction by more than a factor of three, indicating a high degree of sensitivity to the value of R_{edge}, as expected. By the end of these simulations, essentially all the particles that are being lost have been fully thermalised, i.e., they have energies of the order of the temperature close to the plasma edge. Theoretically-calculated diffusivities for particles of a given species are strongly-increasing functions of particle velocity in both the ripple-plateau[3] and collisional ripple well trapping[21] regimes. Hence ripple transport is predicted to be much lower for thermalised ions than it is for energetic ions, and therefore we would not expect the figures in Table I to rise significantly with longer simulation times. Indeed calculations of the power loss fraction based solely on losses occurring in the first 30 ms of each simulation yield similar results.

TABLE I. Ripple-induced loss of beam power in MAST-like plasmas.

R_{edge} (m)	Power loss fraction (%)
1.37	0.29
1.44	0.80
1.51	2.80

IV. CONCLUSIONS AND DISCUSSION

We have used a full orbit test-particle approach to determine the transport of beam ions due to toroidal ripple in MAST, taking into account collisional interactions with electrons and bulk ions. For a typical MAST plasma, we have estimated the anomalous diffusivity arising from ripple effects to be at most 0.1 m^2 s^{-1}, indicating that such effects cannot account for the bulk of the anomalous transport ascribed to beam ions in MAST. Despite the relatively high Larmor radii of beam ions in MAST, there are no indications that finite Larmor radius effects cause a significant increase in ripple transport. Analysis of the distributions of losses in energy and poloidal angle, indicating that delayed losses mostly occur close to the midplane, suggests that the ripple-induced losses are most likely to be due to banana-drift diffusion, with ripple trapping playing little or no role. We have also found that the power loss fraction due to ripple transport depends sensitively on the major radius of the outer midplane plasma edge R_{edge}, rising to more than 2% when $R_{edge} \simeq 1.5$ m.

The fact that there is no evidence of cyclotron resonance effects causing an enhancement of beam ion ripple transport in MAST is somewhat counter to expectations (cf. Sec. I) and therefore merits further discussion. Almost all of the beam ions lying close to the last closed flux surface in MAST are deeply trapped, due to a combination of the beam deposition profile, the birth velocities of the beam ions, and the low aspect ratio of the plasma edge, which causes the magnetic field on this surface to vary by more than a factor of four. The poloidal distributions of lost particles shown in Figs. 5 and 6 reflect, to a large extent, the poloidal distributions of confined beam ions lying close to the last closed flux surface; there are very few beam ions in the vicinity of the inner plasma boundary. Putvinskii and Shurygin[22] demonstrated that the critical ripple amplitude above which particle trajectories become stochastic due to cyclotron resonance tends to zero at the trapped-passing boundary for particles with $v_\parallel > v_{\parallel *} \equiv \Omega_i / k_\parallel$. However as the ripple amplitude decreases, the width of the stochastic region of pitch angle space also decreases, as does the associated particle diffusivity.[22] In MAST, almost all the energetic beam ions lying close to the trapped-passing boundary are deep inside the plasma, where the ripple amplitude is very small (e.g., $\delta \sim 10^{-4}$ at $R = 1$ m). This implies that cyclotron resonance effects are in fact unlikely to be contributing significantly to the beam ion ripple losses. It should be noted that this conclusion does not necessarily apply to fusion α-particles in burning plasma spherical tokamaks, since, unlike beam ions in MAST, these will have almost isotropic velocity distributions.[7]

The fact that ripple cyclotron resonance interactions are restricted to a limited range of pitch angles raises the issue of whether the numbers of test particles used in our simulations (10 000-28 000) are sufficient to represent such interactions. The energies, toroidal canonical momenta, and magnetic moments of the simulated test particles are not conserved since they are being tracked on collisional slowing-down timescales (30–90 ms) in non-axisymmetric fields. Thus, a significant proportion of the particles would be expected to have $v_\parallel > v_{\parallel *}$ and pitch angles close to the local trapped-passing boundary at some point in their trajectories, and any effect of the cyclotron resonance on ripple transport should therefore be reflected in the recorded particle loss rate. However, as noted above, essentially all beam ions passing through the outboard plasma edge in MAST (the only region of the plasma where the ripple amplitude is high enough to significantly affect fast particle transport) are deeply trapped and are therefore unaffected by the cyclotron resonance.

The sensitivity of ripple losses to the value of R_{edge} should be taken into account in any plans to operate large plasmas in MAST, although it is important to note that any non-ambipolar loss of energetic particles from a tokamak plasma quickly leads to the establishment of a radial return current, carried by either bulk or impurity ions, the Ohmic dissipation of which at least partly compensates for the reduction of direct collisional heating arising from the loss of beam ions.[23] Indeed MAST plasmas with counter-current NBI, and hence a very high rate of prompt beam ion losses, have been observed to have energy confinement times higher than those of comparable plasmas with co-injection.[24] The Lorentz force associated with the return current also causes counter-current toroidal rotation, which in turn produces an inward-directed radial electric field;[23] the formation of strongly-negative radial electric fields has been found in MAST to be closely correlated with transitions from low to high confinement regimes.[25] Moreover, the production of a significant counter-current torque by enhanced ripple losses has been clearly demonstrated in the Joint European Torus (JET) experiment.[26] Thus, there are reasons to believe that non-ambipolar ripple losses could in fact have beneficial effects on plasma confirement.

As noted in Sec. I, this study was motivated in part by a desire to identify a mechanism for the anomalous beam ion transport in MAST reported in Ref. 8. The choice of strategies for reducing this transport depends on what is causing it. One could, for example, attempt to minimise or eliminate fast particle transport due to fishbone instabilities by reducing the plasma current (i.e., increasing the plasma safety factor q) to avoid this particular class of instability. Such an approach is likely to increase ripple losses, since these are generally greater in advanced scenario plasmas with high central q,[11] and there is evidence of a correlation between beam ions losses and q in MAST.[9] However, for typical MAST values of R_{edge}, the level of ripple losses is sufficiently low that somewhat higher levels could perhaps be tolerated, particularly in view of the possible beneficial effects of such losses noted above.

ACKNOWLEDGMENTS

This work was funded by the RCUK Energy Programme under Grant EP/I501045, by the Australian Research Council, and by the European Communities under the Contract of Association between EURATOM and CCFE. The authors are grateful to Dr. Colin Roach (CCFE) for providing the axisymmetric component of the equilibrium used in Sec. III, to Dr. Rob Akers (CCFE) for simulating the birth positions of beam ions, and to Dr. Michael Fitzgerald (Australian

National University) for providing assistance with the computations. The views and opinions expressed herein do not necessarily reflect those of the European Commission.

[1]G. Manfredi and R. O. Dendy, Phys. Rev. Lett. **76**, 4360 (1996).
[2]B. N. Breizman and S. E. Sharapov, Plasma Phys. Controlled Fusion **37**, 1057 (1995).
[3]R. J. Goldston and H. H. Towner, J. Plasma Phys. **26**, 283 (1981).
[4]F. L. Hinton, Plasma Phys. **23**, 1143 (1981).
[5]S. V. Putvinskii, JETP Lett. **36**, 397 (1982).
[6]P. N. Yushmanov, Rev. Plasma Phys. **16**, 117 (1990).
[7]K. G. McClements, Phys. Plasmas **12**, 072510 (2005).
[8]M. Turnyanskiy D. L. Keeling, R. J. Akers, G. Cunningham, N. J. Conway, H. Meyer, C. A. Michael, and S. D. Pinches, Nucl. Fusion **49**, 065002 (2009).
[9]M. Valovič, R. Akers, M. de Bock, J. McCone, L. Garzotti, C. Michael, G. Naylor, A. Patel, C. M. Roach, R. Scannell, M. Turnyanskiy, M. Wisse, W. Guttenfelder, J. Candy, and MAST team, Nucl. Fusion **51**, 073045 (2011).
[10]T. C. Hender, A. Bond, J. Edwards, P. J. Karditsas, K. G. McClements, J. Mustoe, D. V. Sherwood, G. M. Voss, and H. R. Wilson, Fusion Eng. Des. **48**, 255 (2000).
[11]S. V. Konovalov, E. Lamzin, K. Tobita, and Yu. Gribov, in *Proceedings of the 28th EPS Conference on Controlled Fusion and Plasma Physics*, edited by C. Silva, C. Varandas, and D. Campbell (European Physical Society, Petit-Lancy, 2001), Vol. 25A, p. 613.
[12]A. W. Morris, R. J. Akers, G. F. Counsell, T. C. Hender, B. Lloyd, A. Sykes, G. M. Voss, and H. R. Wilson, Fusion Eng. Des. **74**, 67 (2005).
[13]V. Yavorskij, A. Moskvitin, Yu. Moskvitina, V. Goloborod'ko, and K. Schoepf, Nucl. Fusion **50**, 084022 (2010).
[14]B. Hamilton, K. G. McClements, L. Fletcher, and A. Thyagaraja, Sol. Phys. **214**, 339 (2003).
[15]B. A. Trubnikov, Rev. Plasma Phys. **1**, 105 (1965).
[16]C. W. Gardiner, *Handbook of Stochastic Methods*, 2nd ed. (Springer-Verlag, Berlin, 1985), pp. 96–97.
[17]P. Helander and D. J. Sigmar, *Collisional Transport in Magnetized Plasmas* (Cambridge University Press, Cambridge, 2002), pp. 35–38.
[18]R. J. McKay, K. G. McClements, A. Thyagaraja, and L. Fletcher, Plasma Phys. Controlled Fusion **50**, 065017 (2008).
[19]D. J. Applegate, C. M. Roach, S. C. Cowley, W. D. Dorland, N. Joiner, R. J. Akers, N. J. Conway, A. R. Field, A. Patel, M. Valovic, and M. J. Walsh, Phys. Plasmas **11**, 5085 (2004).
[20]D. Stork, Fusion Eng. Des. **14**, 111 (1991).
[21]T. E. Stringer, Nucl. Fusion **12**, 689 (1972).
[22]S. V. Putvinskii and R. V. Shurygin, Sov. J. Plasma Phys. **10**, 534 (1984).
[23]K. G. McClements and A. Thyagaraja, Phys. Plasmas **13**, 042503 (2006).
[24]R. J. Akers, P. Helander, A. Field, C. Brickley, D. Muir, N. J. Conway, M. Wisse, A. Kirk, A. Patel, A. Thyagaraja, and C. M. Roach, and MAST and NBI Teams, in *Proceedings of the 20th IAEA Fusion Energy Conference* (International Atomic Energy Agency, Vienna, 2005), EX/4-4.
[25]H. Meyer, R. J. Akers, F. Alladio, L. C. Appel, K. B. Axon, N. Ben Ayed, P. Boerner, R. J. Buttery, P. G. Carolan, D. Ciric, C. D. Challis, I. T. Chapman, G. Coyler, J. W. Connor, N. J. Conway, S. Cowley, M. Cox, G. F. Counsell, G. Cunningham, A. Darke, M. deBock, G. deTemmerman, R. O. Dendy, J. Dowling, A. Yu Dnestrovskij, Yu. N. Dnestrovskij, B. Dudson, D. Dunai, M. Dunstan, A. R. Field, A. Foster, L. Garzotti, K. Gibson, M. P. Gryaznevich, W. Guttenfelder, N. C. Hawkes, J. Harrison, P. Helander, T. C. Hender, B. Hnat, M. J. Hole, D. F. Howell, M. Duc Hua, A. Hubbard, M. Istenic, N. Joiner, D. Keeling, A. Kirk, H. R. Koslowski, Y. Liang, M. Lilley, S. Lisgo, B. Lloyd, G. P. Maddison, R. Maingi, A. Mancuso, S. J. Manhood, R. Martin, G. J. McArdle, J. McCone, C. Michael, P. Micozzi, T. Morgan, A. W. Morris, D. G. Muir, E. Nardon, G. Naylor, M. R. OBrien, T. OGorman, A. Patel, S. D. Pinches, J. Preinhaelter, M. N. Price, E. Rachlew, D. Reiter, C. M. Roach, V. Rozhansky, S. Saarelma, A. Saveliev, R. Scannell, S. E. Sharapov, V. Shevchenko, S. Shibaev, H. Smith, G. E. Staebler, D. Stork, J. Storrs, A. Sykes, S. Tallents, P. Tamain, D. Taylor, D. Temple, N. Thomas-Davies, A. Thornton, A. Thyagaraja, M. R. Turnyanskiy, J. Urban, M. Valovič, R. G. L. Vann, F. Volpe, G. Voss, M. J. Walsh, S. E. V. Warder, R. Watkins, H. R. Wilson, M. Windridge, M. Wisse, A. Zabolotski, S. Zoletnik, O. Zolotukhin, and MAST and NBI teams, Nucl. Fusion **49**, 104017 (2009).
[26]P. C. de Vries, A. Salmi, V. Parail, C. Giroud, Y. Andrew, T. M. Biewer, K. Crombé, I. Jenkins, T. Johnson, V. Kiptily, A. Loarte, J. Lönnroth, A. Meigs, N. Oyama, R. Sartori, G. Saibene, H. Urano, K.-D. Zastrow, and JET EFDA Contributors, Nucl. Fusion **48**, 035007 (2008).